Ray-Based Stochastic Inversion for Reservoir Parameters using 1D Convolutional Forward Modeling

Dennis van der Burg[*†]*, Arie Verdel* [◦]*, and Kees Wapenaar*[†]*,* [◦]*Shell EP Technology,* [†]*Delft University of Technology*

Summary

Ray-Based Stochastic Inversion (RBSI) was introduced in Verdel et al. (2004) as a new seismic inversion method for reservoir parameter estimation claimed to be more accurate than conventional Stochastic Inversion (SI) in laterally heterogeneous subsurfaces. In this paper, an RBSI-variant is presented which utilises a 1D convolutional forward-modeling kernel as found in common inversion software, offering great practical benefits. Synthetic datatests demonstrate the superiority of this variant, in its proper application regime, over SI in resolving reservoir-layer- P-velocities and thicknesses in strongly dipping subsurface structures. SI, under those circumstances, is severely affected by wavelet distortion due to migration.

Introduction

Reservoir parameter estimation in a laterally variable subsurface requires specular reflection-angle- and ray path-information to determine the local reflection-coefficient. A common way to estimate reservoir rock- and pore-fluid- parameters including associated uncertainties, is to perform SI in the reservoir zone on the migrated image, with the migration procedure, see e.g. Schleicher et al. (1993), taking into account the wave propagation path effects through the subsurface given a coarse subsurface velocity macro-model. However, it must be realised that the migrated image is only a bandlimited image of subsurface reflection-coefficients in the case of preserved-amplitude (TA) type migration, a depth migration method which corrects for amplitude losses along the ray due to geometrical spreading as well as interface-transmissions. Also, SI has to deal with wavelet distortion as a result of migration (Tygel et al., 1994). Moreover, on the migrated image, reflection-angle information is often blurred (Levin, 1998) by pre-processing steps, such as angle-range substacks, applied for the sake of enhancing signal-to-noise ratios. For a laterally strongly varying, fine-layered target reservoir sequence, we propose to employ the original ray-path and reflection-angle information, contained in the pre-stack unmigrated data, inside the inversion algorithm, in order to obtain a more accurate reflection amplitude representation in the target zone and hence a more accurate description of reservoir parameter distributions. Exactly this is done in RBSI.

The main difference between RBSI and SI is the inversion-domain. In RBSI inversion is done directly on the pre-stack unmigrated dataset. However, RBSI still needs the depth migrated data to pick the reflector normal vector fields, because in the pre-stack unmigrated domain, RBSI uses 3D elastodynamic ray-tracing as a forward modeller. In this way RBSI takes into account reflection-angle- and ray path-information, whereas in SI 1D convolutional modelling relies on the preceding external process of migration to do that.

RBSI has been successfully applied on synthetic data for the determination of laterally varying layer-densities (Verdel et al., 2004). In this paper, a way is shown in which the scheme can be tuned to estimate P-velocities and layer thicknesses from the wavelet-interfered seismic response of a strongly dipping target reservoir sequence, which behaves locally as a sequence of plane-parallel thin layers.

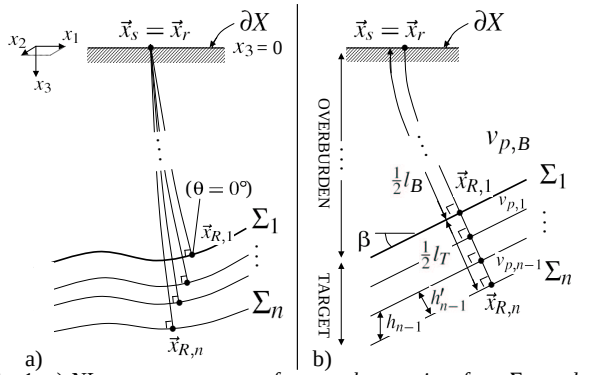

Fig. 1: a) *NI-rays to a sequence of n smooth target interfaces* Σ_i*; angles of incidence* θ*=0°, source- and receiver-position* $\vec{x}_s$*=*$\vec{x}_r$ *at the surface* ∂X*.* b) *Subsurface parameterisation for Reduced RBSI.*

Reduced RBSI

For a sequence of smooth target interfaces of arbitrary shape (Fig. 1a), the seismic normal-incidence (NI) response recorded by a single receiver at the surface will contain information about specular reflection points $\vec{x}_{R,i}$ associated with, generally, non-overlapping ray-paths. Since the true 3D forward modelling must be employed to correctly invert for reservoir parameters of a 3D subsurface model, 1D forward modelling will generally be inadequate. If in the target zone on the NI-dataset nevertheless a 1D convolutional forward modelling engine would be used, as found in common inversion software, refraction, transmission and spreading effects are all not properly taken into account. However, it will be shown that, under certain conditions, employment of a 1D forward modelling kernel in a 'reduced' RBSI scheme - offering great practical advantages - can be a good approximation of the, generally 3D, RBSI-scheme. These conditions are: the target interval behaves locally as plane-parallel layers, contains a moderate amount of layers with not too large impedance contrasts, and has a total interval thickness of, at most, a few wavelengths. In this Reduced RBSI-scheme, amplitude effects of the complex overburden are removed from the NI-data in a pre-processing step, before applying inversion.

We assume, for Reduced RBSI, that the target behaves locally as a sequence of plane-parallel layers (Fig. 1b), and can be identified by a clearly distinguishable reflector, the reference reflector: for convenience, we take Σ_1. Layer- dip angle is β, thicknesses are $h_i < \lambda_d$, with λ_d the dominant wavelength. h_i, $h'_i = h_i \cos\beta$ are the vertical and real thicknesses, respectively.

1D Convolutional Ray-Based Stochastic Inversion

The two-way pathlengths through overburden and target are l_B and l_T ($l_B \gg l_T$). Overburden P-velocity- and density- macro-models $v_{p,B}(\vec{x})$, $\rho_B(\vec{x})$ are assumed known; layer P-velocities and densities in the target are $v_{p,i}$, ρ_i. In this paper, only surface-recorded zero-offset single P-reflections from a 2.5D subsurface are discussed.

Theory

Consider the simple 2.5D caustic-free elastic subsurface model of Fig. 1b, with $v_s = v_p/1.7$ in the target. Density is considered constant throughout the model. The x_3-component of the primary NI P-wave reflection response of the n-th contrast Σ_n in the target, due to an isotropic point source $S(\vec{x},t) = F_0(t)A_0(\vec{x}_s)\delta(\vec{x}-\vec{x}_s)$, with A_0 the source strength and F_0 the wavelet, can be calculated using the expression (founded on the high-frequency Asymptotic Ray Theory):

$$u_3^{(0)}(\vec{x}_s=\vec{x}_r,\vec{x}_{R,n}) = C_B(\vec{x}_s,\vec{x}_T)R^+(\vec{x}_{R,n},\theta=0)\times T_{n-1}(\vec{x}_{R,n},\theta=0)[l_B(\vec{x}_s,\vec{x}_T)+l_T(\vec{x}_T,\vec{x}_{R,n})]^{-1} \quad (1)$$

with $\vec{x}_T$=$\vec{x}_{R,1}$ the intersection point of the NI-ray with Σ_1, dividing the ray-path in parts through overburden and target, C_B the overburden amplitude-effects other than spherical spreading l_B, R^+ the Zoeppritz reflection coefficient measured from the ray-incidence direction, and $T_{n-1} = \prod_{i=1}^{n-1} T_i^-(\theta=0)T_i^+(\theta=0)$ the product of transmission losses in the target (while the ray-pair crosses $n-1$ interfaces through the target; $T_0 := 1$).
The zero-offset particle velocity dataset $\dot{u}_3$ is pre-processed for Reduced RBSI in such a way that all overburden amplitude effects C_B and l_B^{-1} are removed. Amplitude losses within the target, T_{n-1} and l_T^{-1}, are neglected. Note that for a homogeneous isotopic-elastic overburden, $C_B = A_0(\vec{x}_s)C_0(\vec{x}_s,\vec{x}_T)$, with C_0 the free surface correction factor.

SI requires TA Pre-Stack Depth Migration of $\dot{u}_3$, given by [modified from (Schleicher et al., 1993)]:

$$\langle\, R^+(\vec{x},\theta=0)\,\rangle = -\frac{2}{\pi T(\vec{x},\theta=0)}\times \int_{-\infty}^{\infty}\int_{-\infty}^{\infty}\frac{1}{v_p(\vec{x}_r)}\frac{\partial}{\partial t}\dot{u}_3(\vec{x}_r;\,t)|_{t=t_d}\mathrm{d}x_{1r}\mathrm{d}x_{2r} \quad (2)$$

in which t_d represents the two-way time between $\vec{x}$ and $\vec{x}_s=\vec{x}_r$, T takes into account target *and* overburden transmission losses, and "$\langle\,\rangle$" denotes that R^+ is spatially bandlimited.

Regardless of the employed migration algorithm, wavelet distortion occurs on the migrated image. This distortion is a consequence of varying reflection angle, reflector dip and/or velocity. For migrated primary P-P reflection data in a 2.5D setting, the governing expression that measures wavelet stretch in the vertical direction is (Tygel et al., 1994),

$$m_0(v_p(\vec{x}),\theta,\beta) = \frac{2}{v_p}\cos\theta\cos\beta \quad (3)$$

with m_0 the ratio between the wavelet length in the two-way recording time domain and the length in the depth domain, $v_p(\vec{x})$ the local P-wave velocity, θ the angle of ray-incidence and β the local reflector dip. For blocky velocity models, the stretch-evaluation point $\vec{x}$ on the depth migrated image must be chosen just above or below the velocity discontinuity. For a reflector on a zero-offset depth migrated image, the stretch induced by a reflector dip β_0 at position $\vec{x}_A$, relative to the stretch at point $\vec{x}_B$ with zero dip, is given by,

$$n_0'(\beta_0) = \frac{m_0(v_p(\vec{x}_B),\theta=0,\beta=0)}{m_0(v_p(\vec{x}_A),\theta=0,\beta=\beta_0)} = \frac{v_p(\vec{x}_A)}{v_p(\vec{x}_B)}\frac{1}{\cos\beta_0} \quad (4)$$

Conventional inversion, SI, is performed after 1D-depth-to-vertical-two-way-time conversion. In this procedure, a scaling of the migration image along the vertical with local velocity occurs, effectively removing the velocity dependency in the stretch-equation above. This yields the expression for the dip-dependent migration-induced wavelet stretch $n_0(\beta)$ on the depth-to-vertical-time converted migrated image:

$$n_0(\beta) = \frac{1}{\cos\beta} \quad (5)$$

where the subscript for the reflector dip was dropped.

Numerical Examples

Detrimental Effect of Migration Wavelet Stretch $n_0(\beta)$ on SI

To analyse the effect of $n_0(\beta)$ on the ability of conventional inversion, SI, to estimate v_p and h from the migration image [for density-tests see Verdel et al. (2004)], a series of synthetic data tests was performed on a model representing the flank, locally dipping with angle β, of a subsurface structure with a well at the apex (Fig. 2) - simulating a seismic-to-well tie under zero-stretch condition (see Eq. 5). The 2.5D isotropic-elastic subsurface has uniform ρ, constant background v_p = 2000 m/s and contains a single contrasting, thin layer with v_p = 2500 m/s and h =10 m ($< \lambda_d$). The experiments involve SI for unknown layer-properties v_p and h, using the wavelet derived at $\beta = 0^\circ$, on a single trace from a set of TA PreSDM'ed, 1D vertical depth-to-time converted, *ideal* migration images (Fig. 3), each corresponding to a different dip of the flank (all migration artifacts besides the clearly visible wavelet-stretch - the effect considered here - were suppressed). In the construction of these images, the NI-dataset was characterised by a Hanning-tapered zero-phase bandpass wavelet F_0 with corner frequencies 4-12-50-75 Hz. In the experiments, exact mean values (μ_{v_p},μ_h) and the position of Σ_1 were supplied to SI as *prior* layer-knowledge, viz. information available before inversion.

Fig. 4 gives the layer-v_p and -h estimated by SI for the various dip angles. Notice that for higher dip angles, inversion results deviate considerably more than two standard deviations (2σ) from the desired values.
To further investigate these results, consider Fig. 5. In Fig. 5a, one SI-modeled trace (blue) is plotted on top of the corresponding input trace (black varwig) from the migration image (Fig. 3), for each dip angle β. SI-modeled traces provide inversion diagnostics by convolving the most likely SI outcome with the supplied wavelet. Notice that the match with traces from migration is relatively good. In this case, however, the adequate match results in misestimates in v_p and h that stem from positioning-

and amplitude-misalignments due to matching with the wavelet derived at zero-dip. In purple, the traces are displayed without migration stretch: only these traces fulfill the wavelet requirements of SI when using the wavelet derived at zero dip. Fig. 5b, shows for each dip the wavelet that would give correct SI results.

Reduced RBSI vs. SI for layer- P-velocities and thicknesses

In order to test the performance of Reduced RBSI vs. SI, the model was extended to five, plane-parallel, thin layers ($h_i < \lambda_d$) with fixed dip of $\beta = 30^\circ$ (Fig. 6). Fig. 7 shows the datasets on which inversion is applied: on the left, for Reduced RBSI, NI-traces acquired in the subsurface model of Fig. 6, from which overburden amplitude-losses (l_B^{-1} and A_0, C_0 for the homogeneous overburden) are removed. On the right, for SI, the TA PreSDM'ed, 1D depth-to-vertical-time converted, ideal migration image; notice the wavelet stretch.

Fig. 8 gives misestimates in layer-parameters obtained from both types of inversion. Reduced RBSI results are much closer to the desired values than SI results.

Fig. 9a displays on the left an input trace for Reduced RBSI (varwig), from the pre-processed NI dataset of Fig. 7a; the match with the Reduced RBSI-modeled trace (not shown) is almost perfect. The trace on the right shows the difference (scaled by a factor 5 for visibility), causing misestimates, between the input trace and the hypothetical input trace which has losses due to spreading l_T^{-1} and transmission T_{n-1} in the target also corrected for. Note that amplitude errors due to neglect of target amplitude losses are considerably smaller than those occurring by neglect of migration stretch (compare with Fig. 9b, trace on the right, which was not amplified). From Eq. 1, the target amplitude-losses L_l and L_T along the NI-ray, at $\vec{x}_R$ on Σ_6, as compared to $\vec{x}_T$ on Σ_1 read for this configuration:

$$L_l(H) = 1 - \frac{[l_T(\vec{x}_T,\vec{x}_R) + l_B(\vec{x}_s,\vec{x}_T)]^{-1}}{l_B^{-1}(\vec{x}_s,\vec{x}_T)} \quad (6)$$

$$L_T(n) = 1 - T_{n-1}(\vec{x}_R, \theta = 0) \quad (7)$$

with $H = \|\vec{x}_T - \vec{x}_R\| = \Sigma_{i=1}^{n-1} h_i'$. In the chosen model (n=6), L_l and L_T are of the same order, about 0.06 each - values that still give satisfying inversion results (Fig. 8, Red. RBSI). Note also that, due to the fact that L_T should be small in the application regime of Reduced RBSI, the amount of generated multiple-energy too is expected to be small, justifying the choice to model only the primary response in the inversion kernel of Reduced RBSI.

Fig. 9b displays on the left the SI-modeled trace (blue), plotted on top of the corresponding input trace (varwig) from the migration image of Fig. 7b. In purple, the hypothetical ideal input trace without migration stretch is displayed - fulfilling the wavelet requirements of SI when using the wavelet derived at zero-dip. The trace on the right shows the difference, causing SI misestimates, between the real and hypothetical input trace.

Conclusion

Migration stretch severely affects SI and should be accounted for in some way, before inverting for v_p, h, ρ and related reservoir parameters as porosity and pore-fluid content in a strongly dipping target reservoir sequence. Reduced RBSI, a specific implementation of RBSI, however, operates in the pre-stack domain where this stretch is non-existent. The performed synthetic datatests show that Reduced RBSI, in its proper application regime, resolves v_p and h much better than SI. The same has been shown before for RBSI in determining ρ.

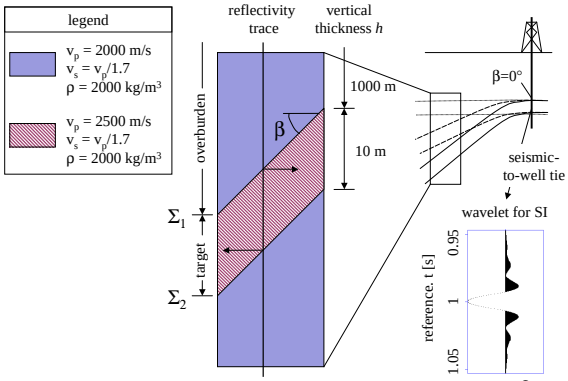

Fig. 2: *Subsurface model with a single v_p-contrast and dip angle β; target layer-v_p and -h to be inverted for. The wavelet for SI was derived from a seismic-to-well tie at zero dip.*

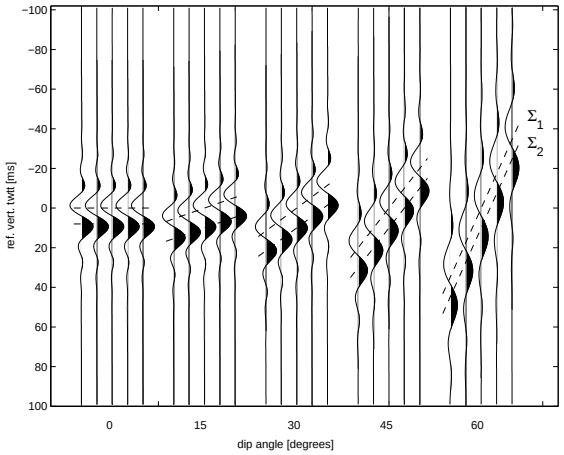

Fig. 3: *$n_0(\beta)$ on a detail of ideal migration results, for the subsurface model of Fig. 2 with dip angle as indicated. Trace separation is 10 m. Dashed lines denote contrasts Σ_i.*

Acknowledgment

The authors wish to thank Shell EP Technology for financially supporting this research and permission to publish this work.

References

Levin, S. A., 1998, Resolution in seismic imaging: Is it all a matter of perspective?: Geophysics, **63**, no. 02s, 743–749.

Schleicher, J., Tygel, M., and Hubral, P., 1993, 3-D true-amplitude finite-offset migration: Geophysics, **58**, no. 08, 1112–1126.

Tygel, M., Schleicher, J., and Hubral, P., 1994, Pulse distortion in depth migration: Geophysics, **59**, no. 10, 1561–1569.

Verdel, A., van der Burg, D., and Wapenaar, K., 2004, Ray-based stochastic inversion:, *in* 66rd Mtg. Eur. Assn. Geosci. Eng., Session: C031.

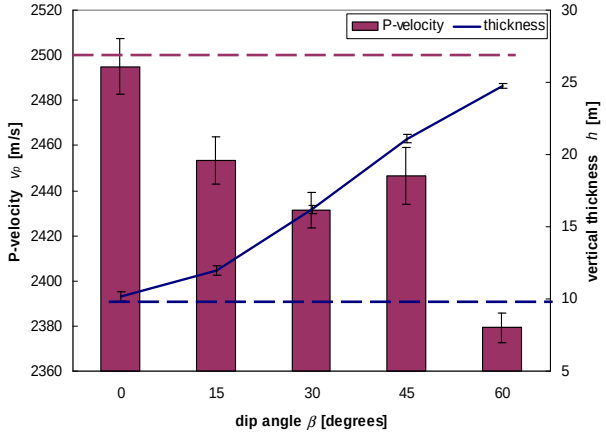

Fig. 4: *v_p and h as determined from SI. Error bars denote σ_{v_p},σ_h. Dashed lines denote desired values, coinciding with prior μ_{v_p},μ_h. Prior σ_{v_p},σ_h were 1000 m/s and 5 m, respectively.*

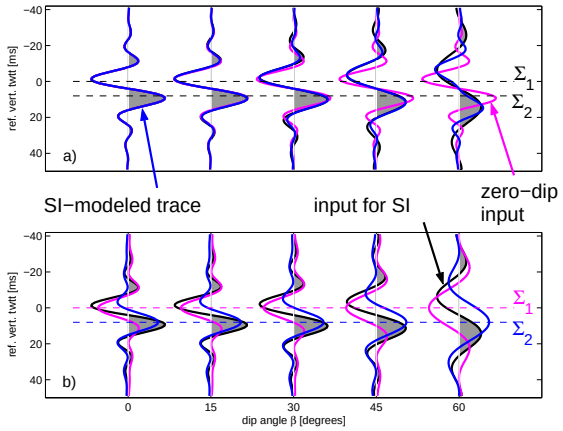

Fig. 5: a) *SI-modeled traces (blue, see text) using the zero-dip wavelet, on SI input traces (black-varwig) from the migration image (Fig. 3). Purple: input at zero-dip.* b) *Migration response per Σ_i, showing the dip-dependent wavelet required for a correct SI.*

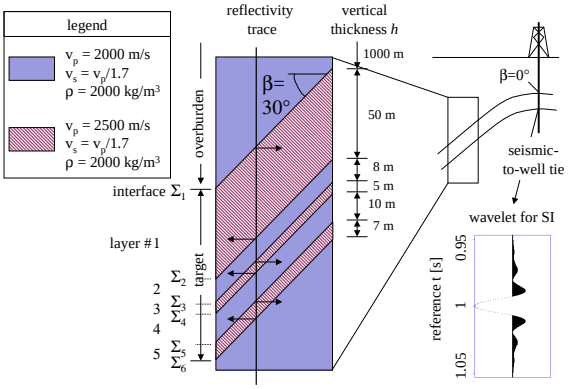

Fig. 6: *Subsurface model with 5 plane-parallel thin layers dipping at $\beta = 30°$; v_p and h to be inverted for. Also shown the wavelet supplied to SI, derived at $\beta = 0°$, and a spiky reflectivity trace.*

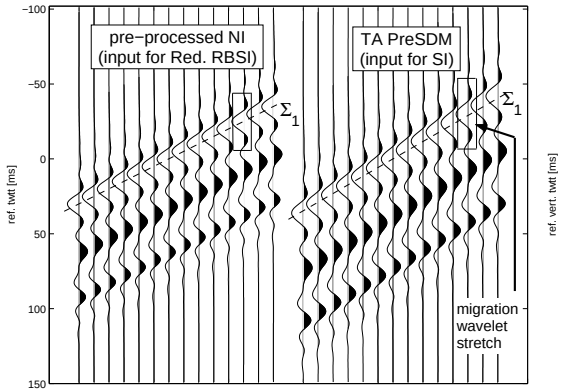

Fig. 7: *Parts of pre-processed NI-data (left, see text) and ideal migration results (right), for the subsurface model of Fig. 6. Trace separation is 10 m. Dashed line denotes reference reflector Σ_1.*

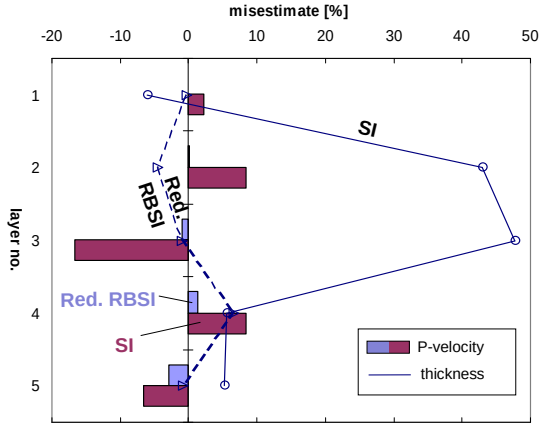

Fig. 8: *misestimates in v_p and h resp. h' determined from SI and the better performing Reduced RBSI. Prior μ_{v_p},μ_h coincide with desired values; prior σ_{v_p},σ_h were 10%.*

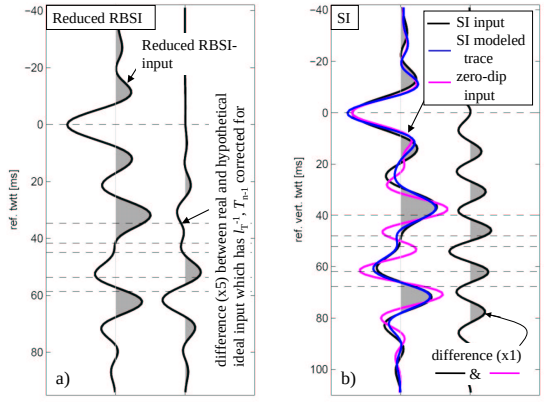

Fig. 9: a) *Reduced RBSI input trace (left) and difference (x5) with ideal input trace.* b) *On the left, on top of each other: SI input, SI-modeled trace and zero-dip input. On the right, difference between real and zero-dip input. Dashed lines denote layer-interfaces.*